ACS APPLIED MATERIALS & INTERFACES

Research Article

www.acsami.org

Electrochemically Controlled Drug-Mimicking Protein Release from Iron-Alginate Thin-Films Associated with an Electrode

Zhiyuan Jin,[†] Güray Güven,[†] Vera Bocharova,*[,†] Jan Halámek,[†] Ihor Tokarev,[†] Sergiy Minko,[†] Artem Melman,[†] Daniel Mandler,[‡] and Evgeny Katz*[,†]

[†]Department of Chemistry and Biomolecular Science, and NanoBio Laboratory (NABLAB), Clarkson University, Potsdam New York 13699-5810, United States

[‡]Institute of Chemistry, The Hebrew University of Jerusalem, Edmond J. Safra Campus, Jerusalem, 91904, Israel

Supporting Information

ABSTRACT: Novel biocompatible hybrid-material composed of iron-ion-cross-linked alginate with embedded protein molecules has been designed for the signal-triggered drug release. Electrochemically controlled oxidation of Fe^{2+} ions in the presence of soluble natural alginate polymer and drug-mimicking protein (bovine serum albumin, BSA) results in the formation of an alginate-based thin-film cross-linked by Fe^{3+} ions at the electrode interface with the entrapped protein. The electrochemically generated composite thin-film was characterized by electrochemistry and atomic force microscopy (AFM). Preliminary experiments demonstrated that the electrochemically controlled deposition of the protein-containing thin-film can be performed at microscale using scanning electrochemical microscopy (SECM) as the deposition tool producing polymer-patterned spots potentially containing various entrapped drugs. Application of reductive potentials on the modified electrode produced Fe^{2+} cations which do not keep complexation with alginate, thus resulting in the electrochemically triggered thin-film dissolution and the protein release. Different experimental parameters, such as the film-deposition time, concentrations of compounds and applied potentials, were varied in order to demonstrate that the electrodepositon and electrodissolution of the alginate composite film can be tuned to the optimum performance. A statistical modeling technique was applied to find optimal conditions for the formation of the composite thin-film for the maximal encapsulation and release of the drug-mimicking protein at the lowest possible potential.

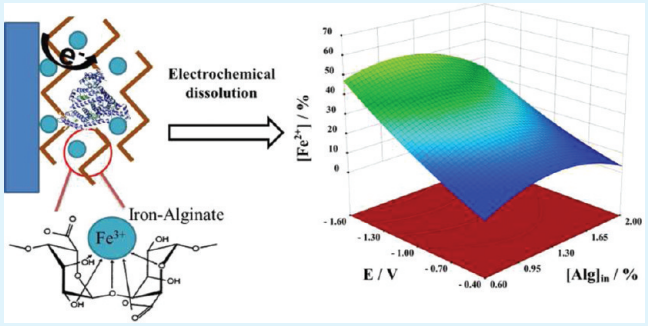

KEYWORDS: *drug release, alginate, electrochemical control, modified electrode, stimuli-responsive electrode*

INTRODUCTION

Novel functional materials for controlled signal-triggered delivery of bioactive substances (drugs, vitamins, nutrients, contrasts for imaging, genes, etc.) recently emerged for various biomedical applications.[1−5] These functional materials based on polymer thin-films,[6−8] membranes,[9] nanoporous[10] and mesoporous structures,[1−3,11,12] capsules,[13−15] and liposomes[16,17] are able to entrap various molecular species and nano-objects and then to release them upon receiving different physical or chemical signals. Signal-responsive systems capable of responding to electrochemically applied potentials,[18−20] magnetic field,[21−25] light signals,[26−28] mechanical signals,[29] temperature changes,[30−33] ultrasound,[34] and chemical/biochemical inputs[35,36] (e.g., pH changes[37−40] or glucose addition[41−43]) were designed and optimized for their operation in vitro[44,45] and in vivo.[46,47] Among methods for preparation of the delivery systems the most frequently used techniques include formation of self-assembled monolayers (SAMs) with direct attachment of active species,[48,49] layer-by-layer (LBL) deposition of polymer molecules with the possibility to incorporate different varieties of entities into molecular assembly[50,51] and encapsulation of entities inside different inorganic or organic nano- or mesoporous materials.[52−54] In the search for suitable matrices for various species encapsulations and then their stimuli release, different signal-responsive polymers[55−57] have been thoroughly investigated.

Alginate, a natural polymer, has attracted researchers owing to its ease of availability, compatibility with hydrophobic as well as hydrophilic molecules, lack of toxicity, and attractive adhesive and mechanical properties.[58] Alginate gels are biodegradable in physiological conditions, and chemically erasable in basic (pH > 7) aqueous environments.[58] Due to the biocompatibility of alginate polymers, they were used for the formation of membranes and thin-films potentially useful in bioseparation and other biorelated applications.[59] Because of alginate ability to be ionically cross-linked with multivalent

Received: November 13, 2011
Accepted: December 26, 2011
Published: December 26, 2011

metal cations entrapping biomolecules into the biopolymer matrix, numerous reports have been published on the encapsulation of proteins/enzymes,[60−62] DNA,[63,64] cells[65,66] and other biomolecular species[67,68] in alginate gels with the retention of their full biological activity. The alginate gel is most notably used as films or microcapsules that can release components passively or in response to changed environmental conditions, through the controlled degradation of the assembly.[69,70] Alternatively, the use of external stimuli allowing for triggering the release of encapsulated species on demand, irrespective of the environmental conditions, is less exploited for alginate in literature.[71] Among various stimuli used for triggering molecular release from signal-responsive matrices,[18−43] the electrochemical triggering is particularly appealing because it enables a precise control over the dissolution process of polymer matrices sensitive to redox transformations.

This control can be achieved through cross-linking of alginate with iron cations which possess distinctly different coordination chemistry of Fe^{2+} and Fe^{3+} cations. Fe^{2+} is a "soft" metal cation that tends to bind neutral ligands containing nitrogen and sulfur atoms, whereas Fe^{3+} cation is a typical example of a "hard" metal cation that preferentially binds oxygen atoms in negatively charged ligands such as carboxylate group.[72] The dramatic difference in binding of carboxylate groups by Fe^{2+} and Fe^{3+} is evident from stability constants of their citrate complexes which have log K_1 values 3.2 and 11.85, correspondingly.[73] Because binding of carboxylate groups by Fe^{2+} is substantially weaker than their binding by Fe^{3+}, it can be expected that "soft" Fe^{2+} cations will have a lower ability for cross-linking alginate in comparison to "hard" Fe^{3+} cations and interconversion between Fe^{2+} and Fe^{3+} will directly affect the alginate gel stability.

Aiming at the electrochemically controlled formation and dissolution of alginate thin-films resulting in the entrapment and release of biomolecules, respectively, we studied Fe^{3+}/Fe^{2+} cross-linking of alginate in the form of thin-films on an electrode surface. Ionic iron can be oxidized and reduced electrochemically as well as used as a cross-linking agent for the formation of alginate gel on an electrode. The advantage of iron ions in comparison to Ca^{2+} (frequently used for alginate cross-linking)[58] is implementing of the electrochemical control over both process of the thin-film formation and dissolution upon changing the iron ions oxidation state. The electrochemical fabrication method provides the possibility of encapsulating proteins in alginate thin-films as a model system for drug delivering.

The present study aims at the detailed investigation of the formation and dissolution of the alginate thin-film cross-linked with iron ions by means of electrochemistry. By changing the composition of the alginate thin-film, electrodeposition time and the applied potential stimulating the film dissolution, the system was optimized for the encapsulation and release of a drug-mimicking protein (bovine serum albumin, BSA). Because of limited information about the mechanism of the controlled protein release and the absence of mathematical models representing complex nature of the process, we applied statistical analyses[74,75] in order to optimize the influence of operational parameters for obtaining the desired responses. Application of multiple regression analysis−response surface methodology (RSM)−was used as a statistical modeling technique employed in the study using quantitative data obtained from properly designed experiments to solve multivariable equations simultaneously.[76] In literature, RSM has been successfully applied for electrodeposition processes,[77,78] whereas in the present paper, it is used for the electrochemically induced release process.

EXPERIMENTAL SECTION

Materials and Instruments. Alginic acid sodium salt from brown algae (medium viscosity, ≥ 2,000 cP), albumin from bovine serum (BSA), sodium sulfate (anhydrous, 99%), ferrous sulfate heptahydrate, Bradford reagent, protein standard (BSA, 200 mg mL^{-1}) and 1,10-phenanthroline monohydrate were purchased from Sigma-Aldrich, J. T. Baker and Fisher Scientific and used as supplied without any pretreatment or further purification. All experiments were carried out in ultrapure water (18.2 MΩ cm; Barnstead NANOpure Diamond).

All electrochemical measurements were performed in 3-electrode system; graphite rod (diameter 3 mm, low density, 99.99% trace metals basis; Sigma-Aldrich), working electrode // Ag|AgCl|KCl 3 M (Metrohm), reference electrode // Pt wire (Metrohm), counter electrode. A single-compartment cell was used with an electrochemical workstation (ECO Chemie Autolab PASTAT 10) and the GPES 4.9 (General Purpose Electrochemical System) software. Micropatterning electrochemical deposition experiments were conducted by a PC-controlled SECM bipotentiostat (CHI920C, CH Instruments Inc., USA) applying the potential pulses in direct-mode. The Pt ultramicroelectrode (UME/10 μm diameter; CHI116, CH Instruments) was positioned by a three-dimensional nanopositioner and acted as a counter electrode in the electrical circuit. A 2-mm Pt substrate, which was used as a working electrode, was polished with 1.0, 0.3, and 0.05 μm alumina powder (Buehler, USA) prior to the experiments. The SECM experiments were carried out with an Ag/AgCl reference electrode and apparatus was placed in a grounded Faraday cage. Images of the deposited microspots were acquired by optical microscopy (Olympus).

Optical absorbance measurements were performed in a 1 mL poly(methyl methacrylate) (PMMA) cuvette with an optical path length of 1 cm using a UV-2450 spectrophotometer (Shimadzu).

Atomic force microscopy (AFM) was used to visualize the film morphology and to perform the scratch analysis of a film thickness. A Dimension 3100 microscope (Veeco Instruments, USA) operating in the tapping mode and BAS-Tap300 Silicon probes (Budget Sensors), having a tip radius of 10 nm, a spring constant of 40 N m^{-1}, and a resonance frequency of 300 kHz, were employed for the analysis. Commercial software supplied with the instrument was used for the image analysis. The composite alginate film for the AFM characterization was prepared electrochemically on a graphite electrode (see the detailed procedure below) and then delaminated from the conducting support by applying potential of −2.0 V for 5 s. A freely floating polymer film was obtained after the electrode was transferred to a plastic tube and gently vortexed. For the AFM measurements the polymer film was placed on a glass slide.

Electrochemical Deposition of Alginate Thin-Films Loaded with BSA on an Electrode. BSA, sodium alginate and $FeSO_4$ were dissolved in 100 mM Na_2SO_4, pH 6.0, and stirred for 4 h at 45 °C. Within the experiments, solutions with different concentrations of each component were prepared by adding 2.5 mg mL^{-1} BSA to different amounts of sodium alginate (0.6, 1.3, and 2.0% w/w) and different concentrations of $FeSO_4$ (5, 20, and 35 mM). BSA-loaded alginate thin-films were deposited on a graphite electrode (geometrical area, 1 cm^2) upon potentiostatic (+0.8 V) oxidation of Fe^{2+} cations resulting in the formation of Fe^{3+} and yielding the alginate cross-linking on the electrode surface. The solutions were degassed by argon purging prior to the electrodeposition. The electrodeposition was performed for 60, 530 and 1000 s and then the modified electrodes were rinsed with water and soaked at room temperature in Na_2SO_4 solution for 45 min prior use. The total amount of the entrapped BSA and cross-linking iron ions was analyzed by dissolution of the thin-films in the presence of ascorbic acid (10 mM) followed by spectrophotometric analysis of the released BSA and Fe^{2+} cations. For the microspot deposition (SECM experiments), the Pt substrate was immersed in the deposition bath containing 100 mM Na_2SO_4 (pH

6.0) supplemented with 1.5% w/w alginate, 5 mM $FeSO_4$ and 1 mM $Ru(NH_3)_6Cl_3$, where the Ru-complex was used as a redox probe for controlling the distance between the UME and Pt surface. Alginate deposition on the Pt surface (E = 0.8 V vs Ag/AgCl) was carried out for 60 s by approaching the substrate with the Pt UME (E = 0 V vs Ag/AgCl). Finally, the modified substrate was washed with copious amount of water.

Electrochemical Release of BSA and Fe^{2+} Cations from the Alginate Thin-Films. BSA and iron ions entrapped in the alginate thin-films were electrochemically released in Na_2SO_4 solution (100 mM, pH 6.0) upon application of reductive potentials (−0.4, −1.0, and −1.6 V) to the modified electrodes for 30 min. Concentrations of the electrochemically released Fe^{2+} cations and BSA were determined spectrophotometrically by standard techniques using 1,10-phenanthroline[79] and Bradford reagent,[80] respectively. Protein standard (Sigma) was used for calibrating the BSA analysis.

Experimental Design and Optimization. Design-Expert 8.0 (Stat-Ease Inc., Minneapolis, USA)[81,82] was employed for regression analysis of the data and optimization (see details in the Supporting Information). The quality of the fit of polynomial model was expressed by the coefficient of determination R^2 and R_{adj}^2, and statistical significance was checked by the F-test in the program. For optimization, a module in Design-Expert software searched for a combination of factor levels that simultaneously satisfy the requirements placed on each of the factors and responses. Performance of the process was evaluated by analyzing the response of electrochemically released product concentrations. The desired goals were selected as maximum electrochemically released Fe^{2+} and BSA concentrations and minimum releasing potential while electrodeposition time, initial Fe^{2+} and alginate concentrations were kept within the range. Corresponding importance of BSA and iron releases were selected as "the most important parameters" in the program. Response surfaces of the objective functions were visualized as 3D plots as a function of two operational factors, while keeping the other two constant at optimum conditions.

All experiments were performed at ambient temperature 23 ± 2 °C.

RESULTS AND DISCUSSION

As can be predicted, "soft" Fe^{2+} cations are much weaker cross-linkers of polysacharide chains in alginate than Fe^{3+} cations. Homogeneous alginate solutions can be obtained with concentration of Fe^{2+} cations up to 40 mM. However, upon their oxidation, Fe^{3+} cations strongly interact with alginate, thus resulting in its cross-linking and gel formation, Figure 1, (quantitative characterization of the alginate gel formation upon reacting in a solution is outside of the scope of the present paper and it will be reported elsewhere).

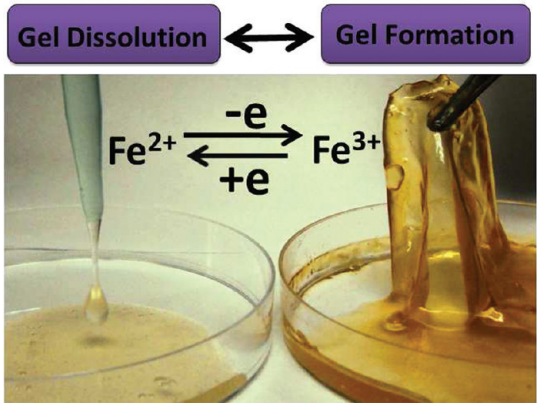

Figure 1. Photograph represents formation of the alginate gel in the solution with Fe^{3+} cations composed of alginate (1.5% w/w), $FeCl_3$ (35 mM) (right), whereas alginate solution with Fe^{2+} cations composed of alginate (1.5% w/w), $FeSO_4$ (35 mM), and 0.1 M Na_2SO_4 remains a viscous liquid (left).

Thin-films of alginate polymer ionically cross-linked with Fe^{3+} cations were produced on graphite electrodes upon electrochemical oxidation of Fe^{2+} ions in the presence of soluble alginate. It should be noted that Fe^{2+} cations originally added to the alginate solution do not result in cross-linking of the alginate, while upon their oxidation, the electrochemically generated Fe^{3+} ions strongly interact with alginate, thus resulting in its cross-linking and deposition on the electrode surface in the form of an insoluble polymer thin-film. When bovine serum albumin (BSA), 2.5 mg/mL, was added to the solution, the electrochemically generated alginate thin-film included physically entrapped BSA which mimicked a protein-drug. Prior to studying the electrochemical dissolution of the alginate thin-film and the corresponding BSA release, the modified electrode coated with the BSA-entrapped/Fe^{3+}-cross-linked/alginate (BSAFeAlg) film was characterized by electrochemistry and atomic force microscopy (AFM). For the electrochemical investigation the modified electrode interface was prepared from a solution containing alginate (1.5% w/w), $FeSO_4$ (35 mM) and 0.1 M Na_2SO_4 as a background electrolyte applying 0.8 V at the graphite electrode for 60 s, whereas for the AFM measurements, the time of the alginate thin-film deposition was varied from 30 to 600 s (see the Experimental Section for the details).

Figure 2 shows cyclic voltammograms obtained on the BSAFeAlg-modified graphite electrode in the solution containing only a background electrolyte. The peaks observed in the

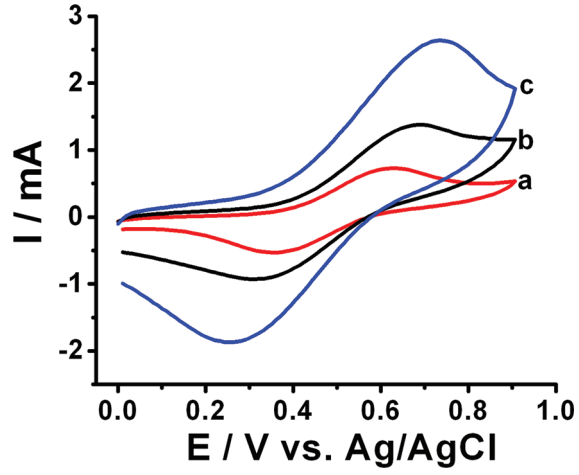

Figure 2. Cyclic voltammograms obtained on the BSAFeAlg-modified graphite electrode in 0.1 M Na_2SO_4 aqueous solution, pH 6; potential scan rates: a) 50, b) 100, c) 150 mV s^{-1}. The BSAFeAlg film was prepared by the electrochemical deposition at 0.8 V for 60 s from the aqueous solution composed of alginate (1.5% w/w), $FeSO_4$ (35 mM), BSA (2.5 mg/mL), and 0.1 M Na_2SO_4.

cyclic voltammograms correspond to the well-defined quasi-reversible redox process of the redox polymer with the midpoint potential of $E_{1/2}$ = 0.495 V. Since the alginate polymer itself is not electrochemically active in the applied potential range (note that Ca^{2+}-cross-linked alginate chemically deposited on an electrode surface in a control experiment does not show any redox peaks in this potential range), the redox process is associated with the reduction/oxidation of iron ions which serve as the cross-linkers in the alginate thin-film. The redox process in the polymer film might be kinetically limited

either by the interfacial electron transfer between the conducting electrode support and adjacent Fe^{3+} species (Laviron-kind kinetics)[83,84] or by the charge propagation across the polymer film (quasi-diffusional kinetics similar to electrochemical diffusional processes in solutions).[85] In order to investigate the kinetics of the electrochemical transformations in the polymer film we recorded cyclic voltammograms at different potential scan rates, ν, Figure 2. The peak-current function on the applied potential scan rate demonstrates a linear dependence, Figure 3A, typical of a nondiffusional electrochemical process, thus indicating that the interfacial electron transfer process of the surface-confined redox species takes place.[83−85] On the other hand, the peak-to-peak separation values, $\Delta E = E_{pa} - E_{pc}$ (where E_{pa} and E_{pc} are potentials of the anodic and cathodic peaks, respectively), derived from the cyclic voltammograms, Figure 3B, are much larger than they might be expected for the surface-confined electrochemistry process, at least for the first Laviron's approximation which predicts zero-value for the ΔE in case of reversible electrochemical reactions.[83] Eventually, the experimental ΔE values are out of the range which allows the quantitative estimation of the interfacial electron transfer rate constants.[83] In other words, the electrochemical process is too slow and the rate constant is too small to be calculated based on the simple Laviron's approach.[83] The ΔE values, larger than expected for the surface-confined electrochemical process, could be also explained by the repulsion interactions between Fe^{3+} species in the frame of the second Laviron's approximation.[84] However, the complexity of this interaction and the lack of the information about many parameters included in the second Laviron's approximation[84] do not allow quantitative analysis of the electrochemical kinetics based on the cyclic voltammetry measurements. The midpoint potential, $E_{1/2}$, derived from the cyclic voltammograms was almost independent of the potential scan rate because the electrochemical process was kinetically symmetrical for the anodic and cathodic reactions: $\delta E_{pa}/\delta(\log \nu) \approx \delta E_{pc}/\delta(\log \nu) \approx 0.33$ V, Figure 3C. Thus, it can be assumed that the anodic and cathodic transfer coefficients α_a and α_c, are both about 0.5, and the experimentally measured $E_{1/2}$ is almost equal to the standard potential E°.[85] This result is interesting and unexpected because the oxidized and reduced iron species, Fe^{3+} and Fe^{2+}, should be in different chemical environment because of their different interaction with the alginate polymer that could possibly lead to different kinetics for their reduction and oxidation processes.

Another unexpected result comes from the comparison of the electrochemically active species contributing to the cyclic voltammetry responses and the total amount of Fe^{3+} species included in the BSAFeAlg film, estimated by full chemical dissolution of the film followed by the chemical analysis of the released Fe^{2+} (see the Experimental Section for details). Surprisingly, integration of the peak-currents in the cyclic voltammograms results in much smaller amount of the redox species than should be if all included in the polymer film Fe^{3+} were electrochemically active. Only 3% of the total content of Fe^{3+} contribute to the cyclic voltammetry response at the potential scan rate of 150 mV s^{-1}, whereas the amount of the electrochemically active Fe^{3+} increases to 9% when the scan rates decreases to 1 mV s^{-1}, still being much smaller than the total content of iron ions in the film. This can be explained by very slow charge propagation across the polymer film, thus resulting in much longer reaction time comparing with the time-scale of the cyclic voltammetry experiments. The thickness

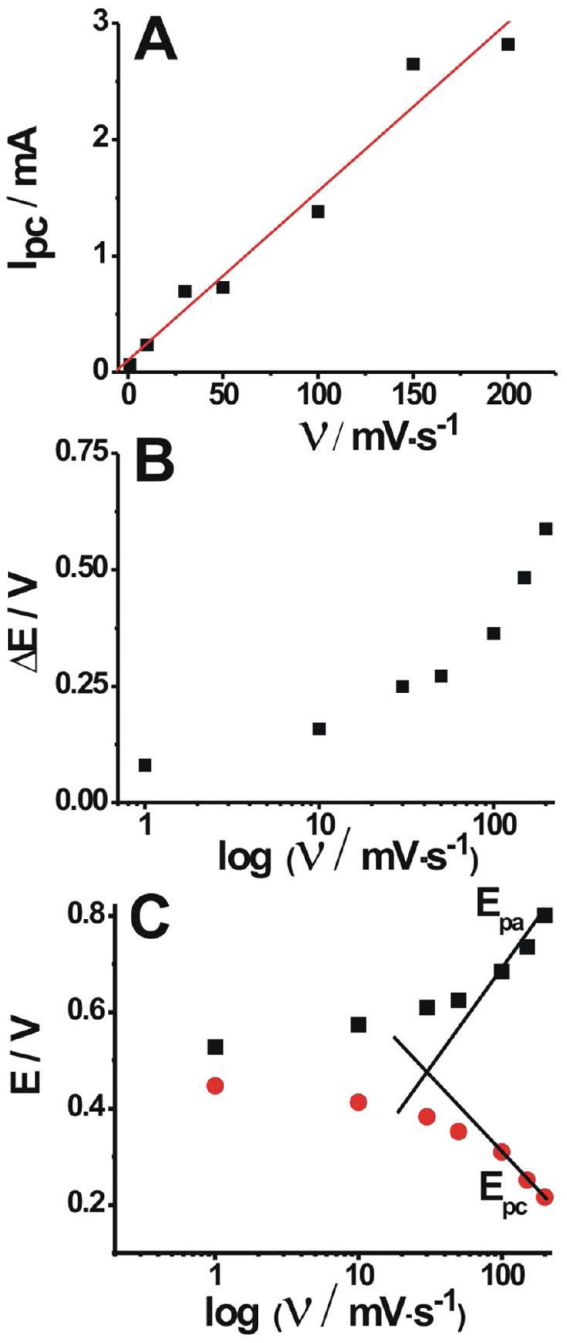

Figure 3. Cyclic voltammetry characterization of the BSAFeAlg-modified electrode: (A) Peak−current (cathodic), I_{pc}, dependence on the potential scan rate, ν. (B) Peak-to-peak separation, ΔE, as function of the potential scan rate, log(ν). (C) Peak current potentials (E_{pa} and E_{pc}, for anodic and cathodic peaks, respectively) as function of the potential scan rate, log(ν). The measurements were performed in 0.1 M Na_2SO_4 aqueous solution, pH 6.0. The BSAFeAlg film was prepared by the electrochemical deposition at 0.8 V for 60 s from the aqueous solution composed of alginate (1.5% w/w), $FeSO_4$ (35 mM), BSA (2.5 mg/mL), and 0.1 M Na_2SO_4.

of the electrochemically responding polymer film (on the time-scale of the cyclic voltammetry experiments) can be estimated as 4.5 and 13.5 nm for ν 150 and 1 mV s^{-1}, respectively (note the total thickness of the polymer film is 150 nm, see the AFM characterization described below). Thus, only the adjacent to the conducting support redox species respond reversibly to the

dx.doi.org/10.1021/am201578m | ACS Appl. Mater. Interfaces 2012, 4, 466−475

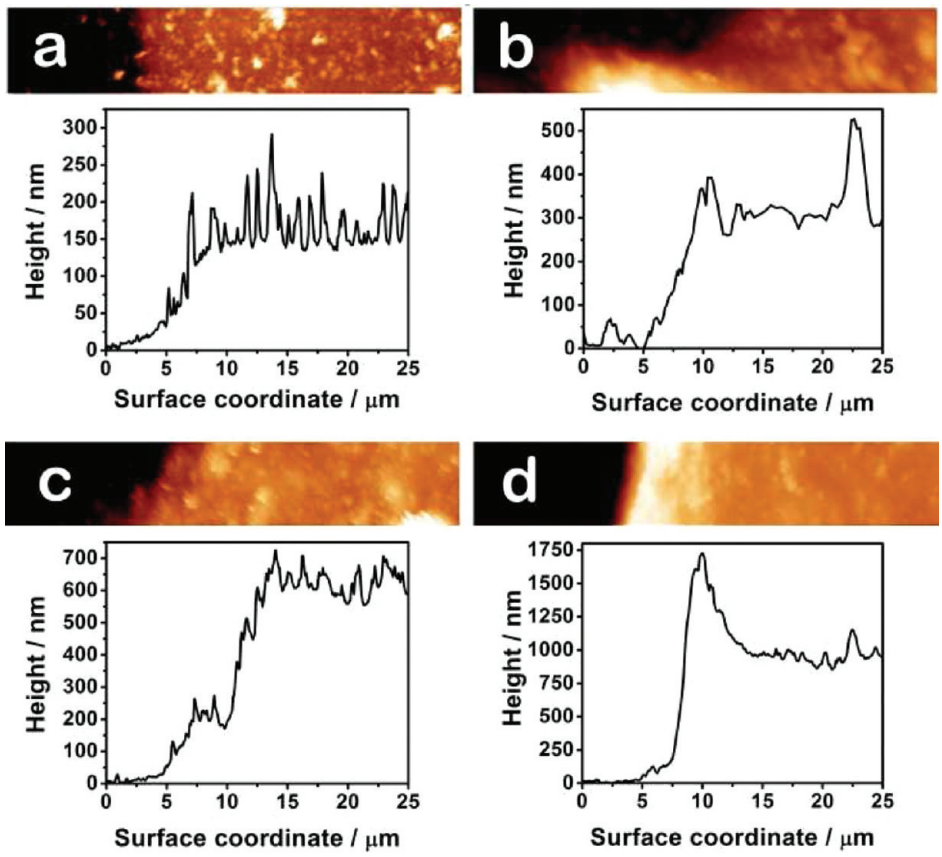

Figure 4. AFM topography images and the corresponding cross-sectional profiles of the BSAFeAlg films electrodeposited for (a) 50, (b) 100, (c) 200, and (d) 400 s from the solution composed of alginate (1.5% w/w), $FeSO_4$ (35 mM), BSA (2.5 mg/mL), and 0.1 M Na_2SO_4 upon application of 0.8 V.

potential changes applied in the cyclic voltammetry experiments, whereas the total redox reaction of the polymeric film requires much longer times and high overpotentials applied to the electrode are needed to facilitate the electron transfer process across the film.

AFM analysis of the electrochemically generated BSAFeAlg films was performed for different deposition-times, Figure 4. To aid the film thickness analysis, we delaminated the films from the graphite substrates, where they were generated electrochemically and transferred onto glass slides; the films were measured near the edges of needle scratches (the dark regions on the images). The measured film thickness clearly increases with the time of the electrochemical deposition, Figure 5. This indicates that the charge propagation across the film is still possible, thus resulting in the continuing growth of the polymer film on the electrode surface upon increasing the deposition time. The polymeric films with larger thicknesses are obviously beneficial for the entrapment of bigger amounts of BSA mimicking an immobilized drug, however, the kinetic problems for the charge propagation found in the electrochemical experiments would limit the efficiency of the BSA electrochemical release from the thick polymer films, thus requiring optimization of the polymer film thickness by varying the deposition time and the film composition.

To demonstrate the spatial selectivity of the BSAFeAlg film formation, the deposition on an electrode surface was performed in the form of a pattern using scanning electrochemical microscopy (SECM).[86,87] The deposition was conducted in the direct mode[88,89] using ultra-micro-electrode

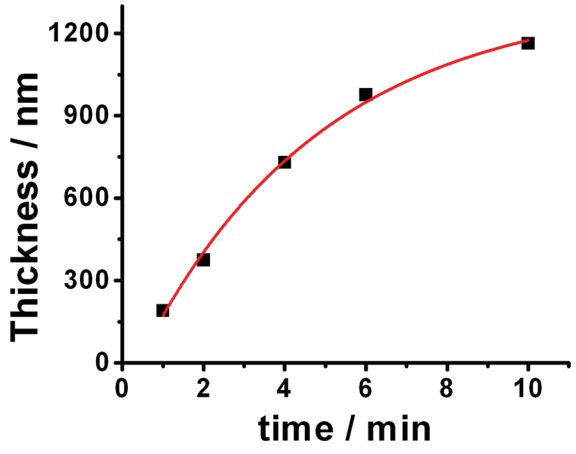

Figure 5. BSAFeAlg film thickness derived from AFM images (similar to Figure 4) as the function of the electrochemical deposition time period.

(UME) and a platinum substrate. The UME was biased at 0 V in a solution of 100 mM Na_2SO_4, pH 6.0, 1.5% w/w alginate, 5 mM $FeSO_4$ and 1 mM $Ru(NH_3)_6Cl_3$ for 60 s; at the same time the substrate was biased at 0.8 V. In our experimental conditions when a UME was brought near a conducting surface (a few micrometers above the substrate surface), electron transfer was confined to a small area resolved by means of optical microscopy as a spot with the lateral dimensions of ca. 250 μm as shown in Figure 6A. Figure 6B shows the electrodeposited spot topography measured by the

dx.doi.org/10.1021/am201578m | ACS Appl. Mater. Interfaces 2012, 4, 466–475

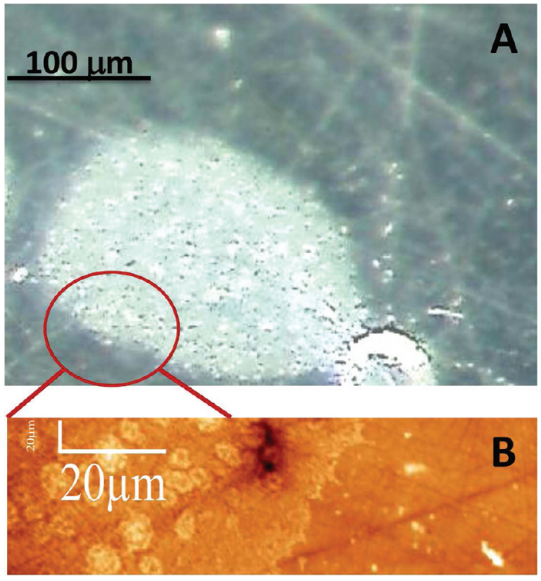

Figure 6. (A) Optical microscope image of the Fe^{3+}-cross-linked alginate microspot produced by SECM on a Pt support from the 100 mM Na_2SO_4, pH 6.0, electrolyte solution containing 1.5% w/w alginate, and 5 mM $FeSO_4$ upon application of 0.8 V for 60 s; 1 mM $Ru(NH_3)_6Cl_3$ was present in the solution as a redox probe for SECM (see details in the Experimental Section). (B) The topography of the electrochemically generated alginate microspot imaged by the AFM.

AFM at the region marked with red in Figure 6A. The spot localized on the surface with sharply defined borders (height ca. 50 nm), giving a distinct topological contrast between the bare electrode and the composite film, confirming spatial confinement of the thin-film in the lateral direction to the electrode. SECM-based surface patterning can be used to form a variety of micrometer-sized structures.[90−92] The use of polymers[91,92] for patterning with SECM is particularly attractive because of the possibility of entrapment of different biological molecules within a polymer film, which could potentially be used for electroaddressing of different biological components at specific device addresses, enlisting the capabilities of electronics to provide spatiotemporally controlled electrochemical signals.

After characterization of the BSAFeAlg films by electrochemistry and AFM, the films were electrochemically dissolved by reducing cross-linking Fe^{3+} to yield Fe^{2+}, which is weakly interacting with alginate, thus resulting in the BSA release, Scheme 1. The chronocoulometry was used to follow the electrochemical reduction process of Fe^{3+} in the polymeric film upon application of various potentials to the modified electrode, Figure 7A. Then the released BSA and Fe^{2+} were chemically analyzed in the solution (see the Experimental Section for the details) to give quantitative measure of the polymer film decomposition by the electrochemical process. In order to find the total amount of BSA entrapped in the alginate thin-film and to characterize the electrochemically released BSA as percentage from this amount, the alginate film was chemically reacted with ascorbic acid (10 mM, 30 min), which resulted in the complete Fe^{3+} reduction and film dissolution. A cyclic voltammogram recorded on the electrode after chemical dissolution of the BSAFeAlg film does not show any redox peaks, thus confirming the complete decomposition of the polymer film. The total amount of BSA encapsulated in the composite film was found to be different for different time of film deposition and varying from 20 to 403 μg that

Scheme 1. Schematic Representation of Electrochemical Dissolution of the BSAFeAlg Film upon Reduction of the Cross-Linking Fe^{3+} Cations Resulting in the Release of BSA and Fe^{2+} Cations into a Solution

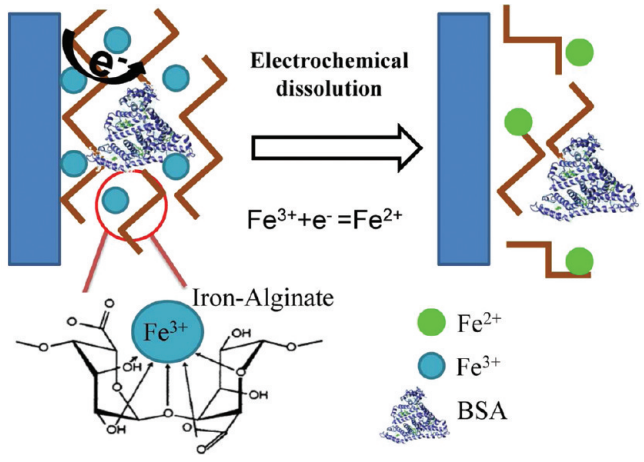

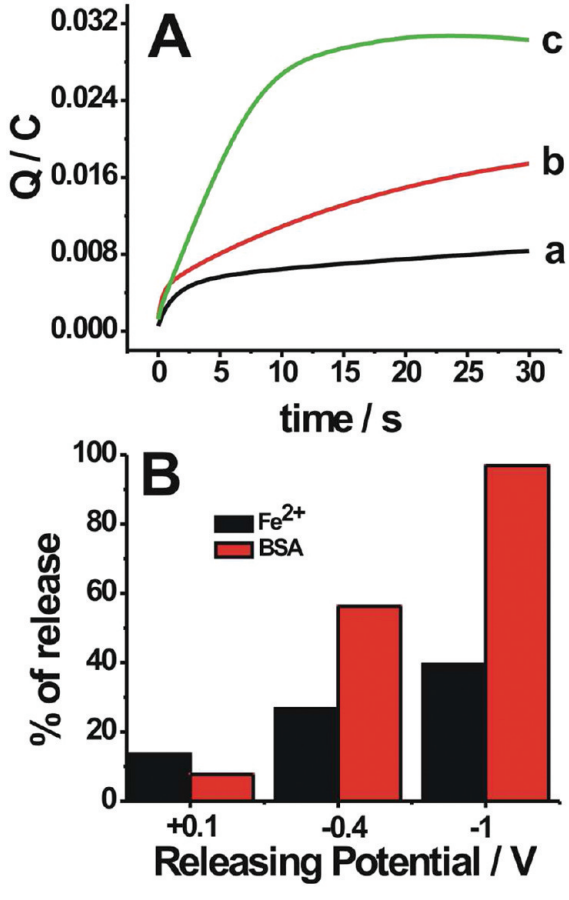

Figure 7. (A) Chronocoulometry curves obtained for the electrochemical dissolution of the BSAFeAlg films upon application of different reductive potentials: (a) +0.1, (b) −0.4, (c) −1.0 V to the modified electrode. (B) Percentage (from the total amount in the BSAFeAlg film) of the released iron cations and BSA upon application of different reductive potentials for 30 min. The BSAFeAlg-film was prepared by the electrochemical deposition at 0.8 V for 60 s from the aqueous solution composed of alginate (1.5% w/w), $FeSO_4$ (35 mM), BSA (2.5 mg/mL) and 0.1 M Na_2SO_4.

dx.doi.org/10.1021/am201578m | ACS Appl. Mater. Interfaces 2012, 4, 466−475

corresponds to ca. 10% (w/w) from the BSAFeAlg film deposited for 60 s. The electrochemical release of BSA performed at different reducing potentials, +0.1, −0.4, and −1.0 V shows increasing BSA release upon elevation of the reductive potential, Figure 7B. It should be noted that all these potentials are thermodynamically enough for the reduction of the cross-linking Fe^{3+} cations in the BSAFeAlg film (note $E°(Fe^{3+}/Fe^{2+})$ = 0.495 V derived from the cyclic voltammograms, Figure 2). However, taking into account the slow charge propagation, the more negative potentials provide the higher rates for the electrochemical dissolution process and the corresponding BSA release, Figure 7B, changing from ca. 10% of the total amount of BSA in the film at the potential of 0.1 V applied for 30 min to almost 100% BSA release when −1.0 V was applied for the same time-period. It should be noted that the time scale of the charge propagation, 30 s, in the chronocoulometry experiment (Figure 7A) and the time required for the polymer film dissolution, 30 min, (Figure 7B) are significantly different. This is not surprising since the former process includes only electron hopping between the Fe^{3+} redox species, while the latter includes dissociation of chemical bonds and decomposition of the polymeric film. When the modified electrode was incubated in an aqueous solution (100 mM Na_2SO_4, pH 6.0) without applied potentials, a small BSA leakage has been detected (ca. 4% per hour on the time scale of 5 h). This process represents the BSA release from the macroporous alginate gel without reduction of Fe^{3+} cross-linking centers and without the gel dissolution. This process depends on the density of the gel, which can be varied and optimized.

Multiparameter optimization was applied to the system in order to find optimum conditions for the BSAFeAlg film electrochemical formation and decomposition. Central composite design (CCD)[93,94] was used for experimental design based on response surface methodology (RSM)[95] in the current study (see details in the Supporting Information). It should be noted that the response surface analysis has been shown as a powerful method in the optimization of drug delivering systems.[96] A quadratic model,[93] which also includes the linear terms, given as eq 1, was used in the present study

$$\eta = \beta_0 + \sum_{j=1}^{k} \beta_j x_j + \sum_{j=1}^{k} \beta_{jj} x_j^2 + \sum_{i} \sum_{<j=2}^{k} \beta_{ij} x_i x_j + e_i \quad (1)$$

where; η is the response, x_i and x_j are variables (i = 1 to k), β_o is the constant coefficient, β_j, β_{jj}, and β_{ij} (i and j = 1 to k) are interaction coefficients of linear, quadratic and the second-order terms, respectively, k is the number of independent parameters (k = 4 in this study) and e_i is the error. The variables (initial concentrations of Fe^{2+} and alginate, releasing potential and electrodeposition time) were chosen as independent (operational) parameters since they are directly related to the operational preference. The process was evaluated by considering electrochemically released Fe^{2+} and BSA concentrations as objective functions. CCD with four factors at three levels was used for fitting experimental data to the objective functions. Optimized conditions with the highest desirability were determined as −1.19 V releasing potential, 35 mM initial Fe^{2+} concentration, 60 s deposition time, and 0.96% initial alginate concentration. Under these optimized conditions, electrochemical release of BSA and iron are 81.22 and 59.83% from their total content in the BSAFeAlg film, respectively. In order to validate the optimization, a specific batch run was performed under the optimum conditions. In this run, electrochemical release of BSA and iron were realized as 85.60% and 51.35%, respectively, providing fair predictive power of the model approach.

Equations derived from the CCD analysis (see eqs 2 and 3 in the Supporting Information) were used to visualize the effects of operational parameters on electrochemical release of Fe^{2+} and BSA under optimized conditions in 3D graphs, Figures 8 and 9 and Figures SI1 and SI2 in the Supporting Information

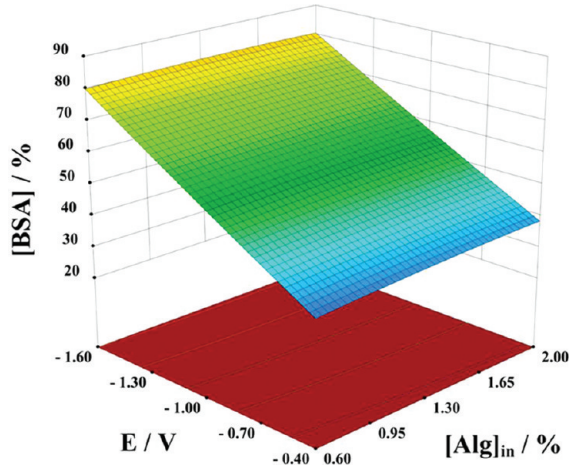

Figure 8. Effects of the releasing potential (E) applied to the BSAFeAlg-modified electrode and initial alginate concentration ($[Alg]_{in}$) on the electrochemically released BSA concentration ([BSA]), at room temperature, 60 s polymer film deposition time, and 35 mM initial Fe^{2+} concentration used for the polymer film deposition.

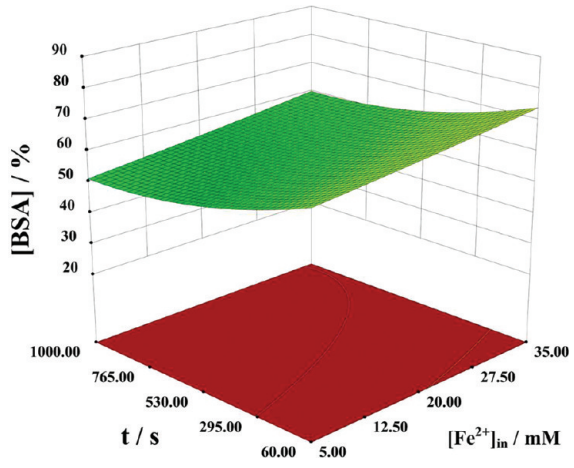

Figure 9. Effects of the deposition time (t) and initial iron concentration ($[Fe^{2+}]_{in}$) on the electrochemically released BSA concentration ([BSA]), at room temperature, −1.19 V releasing potential and 0.96% (w/w) initial alginate concentration used for the polymer film deposition.

(note that the electrochemically induced release of the drug-mimicking protein BSA is the primary aim of the study, thus

dx.doi.org/10.1021/am201578m | ACS Appl. Mater. Interfaces 2012, 4, 466−475

results of the concomitant release of Fe^{2+} cations are collected in the Supporting Information, Figures SI1 and SI2). The effects of the releasing potential and initial alginate concentration on the electrochemical release of BSA and Fe^{2+} are shown in Figure 8 and Figure SI1 in the Supporting Information, respectively. During electrochemical process, released BSA and Fe^{2+} concentrations increased proportionally to the increase in the reductive potential applied on the BSAFeAlg-modified electrode. These data confirm the result derived earlier from the electrochemical measurements that the charge propagation in the alginate film attached to the electrode surface depends on the applied potential. For the condition when the propagation of the charge carriers through the film is sensitive to the applied potential, the choice of the potential range is of high importance. For ultrathin-films, low potentials for the electrochemical release would be sufficient, whereas thicker films require maintaining release at relatively high reductive potentials, where side reactions may become dominant affecting morphology of the membrane. Therefore, the lowest possible potential value able to achieve satisfactory levels of the electrochemical release for relatively thick films within a relatively short period of time should be employed. According to the releasing efficiency and control experiments performed to determine stability of the BSAFeAlg at different potentials, the releasing potential of −1.19 V would be a good choice, where the electrochemical release is relatively sufficient, while the membrane is not deformed or rapidly detached. In general, initial alginate concentration does not profoundly affect the electrochemical release of BSA, Figure 8. On the other hand, electrochemical release of Fe^{2+} decreased with an increase in initial alginate concentration at high alginate concentrations, > 1.3%, see Figure SI1 in the Supporting Information. Relatively high initial alginate concentration provides larger number of binding sites of alginate for iron ions resulting in the formation of a more compact gel membrane as it was previously reported for calcium cross-linked alginate gels,[100] which, in turn, leads to increase in the electrochemical release of Fe^{2+} cations. In our experiments, this situation is realized for concentrations of alginate less than 1.3%, see Figure SI1 in the Supporting Information. Although the concentration of iron remains constant (35 mM) concentration of alginate is increasing reaching values where viscosity is high, so for concentration of alginate more than 1.3% the steric effects in the solution became dominant. Furthermore, disbalance between the amount of binding sites for iron ions in alginate and concentration of iron with the overall high concentration of alginate favored the process of partial blocking the electrode surface preventing iron influx to the electrode, enabling electrochemical formation of thinner film with increased inhomogeneity in the structure.

Effects of deposition time and initial iron concentration on electrochemical release of BSA and iron at room temperature, 0.96% (w/w) initial alginate concentration and −1.19 V releasing potential are shown in Figure 9 and Figure SI2 in the Supporting Information, respectively. A linear increase in the electrochemical release of BSA concentration was observed with the increase on initial iron concentration in the range of 5−35 mM, whereas, electrochemically released iron concentration was increased at relatively high initial iron concentrations (>20 mM). The larger the amount of iron ions reduced in the BSA loaded alginate gel and consequently the larger the amount of the protein released from the membrane by Fe^{2+} ions. When the deposition time is increased the thickness of the membrane increases, and this is presumably due to the fact that increasing the number of biopolymer molecules per unit solution, the number of binding sites for Fe^{2+} ions also increases. As a result a more densely cross-linked gel structure is probably formed, and consequently results in the formation of thicker walls. The dense membrane is expected to create diffusion resistance which resulted in lower release of BSA and iron, Figure 9 and Figure SI2 in the Supporting Information. Moreover, detachment of a thick film (formed at the high deposition time) from the electrode surface was observed during experiments which cause decrease of the electrochemically released amounts of BSA and Fe^{2+}.

■ CONCLUSIONS

Electrochemical formation and decomposition of the iron-ion-cross-linked alginate thin-films was studied as a general approach to the electrochemically triggered controlled drug release process. The concept of the electrochemically responsive alginate films is based on the large difference in the iron ions ability to cross-link alginate depending on the oxidation state of the iron ions. Whereas Fe^{3+} cations result in the alginate gel formation, Fe^{2+} ions have weak interaction with alginate and their electrochemical formation results in the alginate gel dissolution. The electrochemically induced alginate gel formation upon oxidation of iron cations from their original Fe^{2+} state to Fe^{3+} in the presence of soluble alginate was accompanied by entrapment of protein molecules into the gel thin-film structure on the electrode surface. BSA was utilized as a model protein mimicking a drug entrapped in the redox-responsive alginate matrix. The electrochemical reduction of cross-linking Fe^{3+} ions resulted in the alginate gel dissolution and BSA release. The detailed electrochemical study accompanied with AFM characterization of the alginate thin-films revealed kinetic problems for the charge propagation across the polymer films. Therefore, large overpotentials were required for the effective dissolution of the films and BSA release. Multiparameter modeling experiments were performed for the optimization of the redox-responsive polymer film for the effective BSA release. Future efforts will be directed to the facilitation of the charge propagation in the redox-responsive polymer and to the application of real drug molecules for the electrochemically triggered release processes.

It should be emphasized that the use of the alginate matrix results in important advantages for future controlled drug-release applications over other polymer-based systems (particularly comparing with synthetic redox polymers).[18−20] Specifically, the alginate matrix is biocompatible and based on nontoxic natural biomolecules. This matrix is known to stabilize proteins/enzymes resulting in their extended lifetime in the immobilized state.[58]

Still, the issue of the potential toxicity of Fe^{2+} ions[98] released upon electrochemical dissolution of the BSAFeAlg film should be addressed. The concomitant release of Fe^{2+} ions upon complete decomposition of the polymer film results in dissolution of ca. 50 μg iron ions (the exact amount depends on the film composition which could be optimized). This amount should be compared with iron content (10−18 mg daily) in food supplements according to the Recommended Dietary Allowance (RDA) of nutritional elements.[99] One can conclude that the iron release from the BSAFeAlg film is much below the recommended iron consumption, thus there is no any toxicity issue associated with the Fe^{2+} ions.

One should note that BSA is a negatively charged protein at neutral pH values (pI = 4.7),[100] thus its entrapment in the negatively charged[101] alginate gel is unfavorable. The successful results obtained for the entrapment of BSA followed by its controlled release demonstrated that even in this unfavorable combination (negatively charged protein in the negatively charged polymeric matrix) is still possible. Thus, we expect that positively charged proteins (e.g., lysozyme, pI = 11.3)[102] included in the alginate matrix will demonstrate even better performance. The results for a lysozyme–alginate composite film and its antibacterial operation are in progress and will be reported elsewhere.

■ ASSOCIATED CONTENT

Ⓢ Supporting Information

Experimental data and their statistical treatment visualized in the form of 3D plots (PDF). This material is available free of charge via the Internet at http://pubs.acs.org.

■ AUTHOR INFORMATION

Corresponding Author

*E-mail: vbocharo@clarkson.edu (V.B.); ekatz@clarkson.edu (E.K.). Tel.: +1 (315) 268 4421 (V.B.); +1 (315) 268 4421 (E.K.). Fax: +1 (315) 268 6610 (V.B.); +1 (315) 268 6610 (E.K.).

■ ACKNOWLEDGMENTS

This work was supported by the United States–Israel Binational Science Foundation (BSF), Award 2008039. The authors acknowledge the assistance and SECM facilities of Prof. S. Andreescu (Clarkson University).

■ REFERENCES

(1) Aznar, E.; Martínez-Máñez, R.; Sancenón, F. *Expert Opin. Drug Delivery* **2009**, *6*, 643–655.
(2) Santos, H. A.; Salonen, J.; Bimbo, L. M.; Lehto, V. P.; Peltonen, L.; Hirvonen, J. *J. Drug Delivery Sci. Technol.* **2011**, *21*, 139–155.
(3) He, Q.; Shi, J. *J. Mater. Chem.* **2011**, *21*, 5845–5855.
(4) Viseras, C.; Aguzzi, C.; Cerezo, P.; Bedmar, M. C. *Mater. Sci. Technol.* **2008**, *24*, 1020–1026.
(5) Raemdonck, K.; Van Thienen, T. G.; Vandenbroucke, R. E.; Sanders, N. N.; Demeester, J.; De Smedt, S. C. *Adv. Funct. Mater.* **2008**, *18*, 993–1001.
(6) Paun, I. A.; Ion, V.; Moldovan, A.; Dinescu, M. *Appl. Phys. Lett.* **2010**, *96*, No. 243702.
(7) Zelikin, A. N. *ACS Nano* **2010**, *4*, 2494–2509.
(8) Yan, W.; Hsiao, V. K. S.; Zheng, Y. B.; Shariff, Y. M.; Gao, T.; Huang, T. J. *Thin Solid Films* **2009**, *517*, 1794–1798.
(9) Temtem, M.; Pompeu, D.; Jaraquemada, G.; Cabrita, E. J.; Casimiro, T.; Aguiar-Ricardo, A. *Int. J. Pharm.* **2009**, *376*, 110–115.
(10) He, H.; Grignol, V.; Karpa, V.; Yen, C.; LaPerle, K.; Zhang, X.; Jones, N. B.; Liang, M. I.; Lesinski, G. B.; Ho, W. S. W.; Carson, W. E.; Lee, L. J. *J. Controlled Release* **2011**, *151*, 239–245.
(11) Climent, E.; Martínez-Máñez, R.; Sancenón, F.; Marcos, M. D.; Soto, J.; Maquieira, A.; Amorós, P. *Angew. Chem., Int. Ed.* **2010**, *49*, 7281–7283.
(12) Giri, S.; Trewyn, B. G.; Stellmaker, M. P.; Lin, V. S.-Y. *Angew. Chem., Int. Ed.* **2005**, *44*, 5038–5044.
(13) Sukhorukov, G. B.; Rogach, A. L.; Zebli, B.; Liedl, T.; Skirtach, A. G.; Köhler, K.; Antipov, A. A.; Gaponik, N.; Susha, A. S.; Winterhalter, M.; Parak, W. J. *Small* **2005**, *1*, 194–200.
(14) Delcea, M.; Möhwald, H.; Skirtach, A. G. *Adv. Drug Delivery Rev.* **2011**, *63*, 730–747.
(15) Bagaria, H. G.; Wong, M. S. *J. Mater. Chem.* **2011**, *21*, 9454–9466.
(16) Qin, G.; Li, Z.; Xia, R.; Li, F.; O'Neill, B. E.; Goodwin, J. T.; Khant, H. A.; Chiu, W.; Li, K. C. *Nanotechnology* **2011**, *22*, No. 155605.
(17) Adlakha-Hutcheon, G.; Bally, M. B.; Shew, C. R.; Madden, T. D. *Nat. Biotechnol.* **1999**, *17*, 775–779.
(18) Svirskis, D.; Travas-Sejdic, J.; Rodgers, A.; Garg, S. *J. Controlled Release* **2010**, *146*, 6–15.
(19) Boulmedais, F.; Tang, C. S.; Keller, B.; Vörös, J. *Adv. Funct. Mater.* **2006**, *16*, 63–70.
(20) George, P. M.; LaVan, D. A.; Burdick, J. A.; Chen, C.-Y.; Liang, E.; Langer, R. *Adv. Mater.* **2006**, *18*, 577–581.
(21) Pan, D.; Zhang, H.; Fan, T.; Chen, J.; Duan, X. *Chem. Commun.* **2011**, *47*, 908–910.
(22) Panczyk, T.; Warzocha, T. P.; Camp, P. J. *J. Phys. Chem. C* **2010**, *114*, 21299–21308.
(23) Choubey, J.; Bajpai, A. K. *J. Mater. Sci.–Mater. Med.* **2010**, *21*, 1573–1586.
(24) Cai, K.; Luo, Z.; Hu, Y.; Chen, X.; Liao, Y.; Yang, L.; Deng, L. *Adv. Mater.* **2009**, *21*, 4045–4049.
(25) Hu, S.-H.; Tsai, C.-H.; Liao, C.-F.; Liu, D.-M.; Chen, S.-Y. *Langmuir* **2008**, *24*, 11811–11818.
(26) Knežević, N. Ž.; Trewyn, B. G.; Lin, V. S.-Y. *Chem. Commun.* **2011**, *47*, 2817–2819.
(27) Griffin, D. R.; Patterson, J. T.; Kasko, A. M. *Biotechnol. Bioeng.* **2010**, *107*, 1012–1019.
(28) Vivero-Escoto, J. L.; Slowing, I. I.; Wu, C.-W.; Lin, V. S.-Y. *J. Am. Chem. Soc.* **2009**, *131*, 3462–3463.
(29) Lee, K. Y.; Peters, M. C.; Mooney, D. J. *Adv. Mater.* **2001**, *13*, 837–839.
(30) Zhang, W.; Gilstrap, K.; Wu, L.; Bahadur, K. C. R.; Moss, M. A.; Wang, Q.; Lu, X.; He, X. *ACS Nano* **2010**, *4*, 6747–6759.
(31) Fong, W.-K.; Hanley, T. L.; Thierry, B.; Kirby, N.; Boyd, B. J. *Langmuir* **2010**, *26*, 6136–6139.
(32) Chen, S.; Li, Y.; Guo, C.; Wang, J.; Ma, J.; Liang, X.; Yang, L.-R.; Liu, H.-Z. *Langmuir* **2007**, *23*, 12669–12676.
(33) Mathews, A. S.; Cho, W.-J.; Kim, I.; Ha, C.-S. *J. Appl. Polym. Sci.* **2009**, *113*, 1680–1689.
(34) Kapoor, S.; Bhattacharyya, A. J. *J. Phys. Chem. C* **2009**, *113*, 7155–7163.
(35) Richard, D.; Nguyen, I.; Affolter, C.; Meyer, F.; Schaaf, P.; Voegel, J.-C.; Bagnard, D.; Ogier, J. *Small* **2010**, *6*, 2405–2411.
(36) Asai, D.; Kodama, K. B.; Shoji, Y.; Nakashima, H.; Kawamura, K.; Oishi, J.; Kuramoto, M.; Niidome, T.; Katayama, Y. *Med. Chem.* **2008**, *4*, 386–391.
(37) Yuan, L.; Tang, Q.; Yang, D.; Zhang, J. Z.; Zhang, F.; Hu, J. *J. Phys. Chem. C* **2011**, *115*, 9926–9932.
(38) Negrini, R.; Mezzenga, R. *Langmuir* **2011**, *27*, 5296–5303.
(39) Zhang, Z.; Chen, L.; Zhao, C.; Bai, Y.; Deng, M.; Shan, H.; Zhuang, X.; Chen, X.; Jing, X. *Polymer* **2011**, *52*, 676–682.
(40) Aryal, S.; Hu, C.-M. J.; Zhang, L. *ACS Nano* **2010**, *4*, 251–258.
(41) Wang, L.; Liu, M.; Gao, C.; Ma, L.; Cui, D. *React. Funct. Polym.* **2010**, *70*, 159–167.
(42) Gordijo, C. R.; Koulajian, K.; Shuhendler, A. J.; Bonifacio, L. D.; Huang, H. Y.; Chiang, S.; Ozin, G. A.; Giacca, A.; Wu, X. Y. *Adv. Funct. Mater.* **2011**, *21*, 73–82.
(43) Zhao, Y.; Trewyn, B. G.; Slowing, I. I.; Lin, V. S.-Y. *J. Am. Chem. Soc.* **2009**, *131*, 8398–8400.
(44) Rahimi, M.; Wadajkar, A.; Subramanian, K.; Yousef, M.; Cui, W. N.; Hsieh, J. T.; Nguyen, K. T. *Nanomed. Nanotechnol. Biol. Med.* **2010**, *6*, 672–680.
(45) Liu, Y.; Wu, J.; Meng, L.; Zhang, L.; Lu, X. *J. Biomed. Mater. Res. B* **2008**, *85B*, 435–443.
(46) Poon, Z.; Lee, J. B.; Morton, S. W.; Hammond, P. T. *Nano Lett.* **2011**, *11*, 2096–2103.
(47) Sato, Y.; Kawashima, Y.; Takeuchi, H.; Yamamoto, H. *J. Controlled Release* **2003**, *93*, 39–47.
(48) Mani, G.; Johnson, D. M.; Marton, D.; Feldman, M. D.; Patel, D.; Ayon, A. A.; Agrawal, C. M. *Biomaterials* **2008**, *29*, 4561–4573.

(49) Johnson, D. M.; Mahapatro, A.; Patel, D. N.; Feldman, M. D.; Ayon, A. A.; Agrawal, C. M. *Curr. Top. Med. Chem.* **2008**, *8*, 281−289.
(50) Mu, B.; Liu, P.; Du, P.; Dong, Y.; Lu, C. *J. Polym Sci., A* **2011**, *49*, 1969−1976.
(51) Crouzier, T.; Ren, K.; Nicolas, C.; Roy, C.; Picart, C. *Small* **2009**, *5*, 598−608.
(52) Vivero-Escoto, J. L.; Slowing, I. I.; Trewyn, B. G.; Lin, V. S.-Y. *Small* **2010**, *6*, 1952−1967.
(53) De Angelis, F.; Pujia, A.; Falcone, C.; Iaccino, E.; Palmieri, C.; Liberale, C.; Mecarini, F.; Candeloro, P.; Luberto, L.; de Laurentiis, A.; Das, G.; Scala, G.; Di Fabrizio, E. *Nanoscale* **2010**, *2*, 2230−2236.
(54) Zhao, Y.; Vivero-Escoto, J. L.; Slowing, I. I.; Trewyn, B. C.; Lin, V. S.-Y. *Exp. Opin. Drug Delivery* **2010**, *7*, 1013−1029.
(55) Bajpai, A. K.; Shukla, S. K.; Bhanu, S.; Kankane, S. *Prog. Polym. Sci.* **2008**, *33*, 1088−1118.
(56) Bawa, P.; Pillay, V.; Choonara, Y. E.; du Toit, L. C. *Biomed. Mater.* **2009**, *4*, No. 022001.
(57) Traitel, T.; Goldbart, R.; Kost, J. *J. Biomater. Sci.−Polym. Ed.* **2008**, *19*, 755−767.
(58) Donati, I.; Paoletti, S. In *Alginates: Biology and Applications*; Rehm, B. H. A, Ed.; Microbiology Monographs Series; Springer: Dordrecht, The Netherlands, 2009; Vol. *13*, pp 1−53.
(59) Tokarev, I.; Minko, S. *Adv. Mater.* **2009**, *21*, 241−247.
(60) Chan, A. W.; Neufeld, R. J. *Biomaterials* **2010**, *31*, 9040−9047.
(61) Pescosolido, L.; Piro, T.; Vermonden, T.; Coviello, T.; Alhaique, F.; Hennink, W. E.; Matricardi, P. *Carbohyd. Polym.* **2011**, *86*, 208−213.
(62) Barrias, C. C.; Lamghari, M.; Granja, P. L.; Miranda, M. C. S.; Barbosa, M. A. *J. Biomed. Mater. Res., A* **2005**, *74A*, 545−552.
(63) Krebs, M. D.; Salter, E.; Chen, E.; Sutter, K. A.; Alsberg, E. *J. Biomed. Mater. Res., A* **2010**, *92A*, 1131−1138.
(64) Jiang, G.; Min, S.-H.; Oh, E. J.; Hahn, S. K. *Biotechnol. Bioprocess Eng.* **2007**, *12*, 684−689.
(65) Dey, K.; Roy, P. *Biotechnol. Lett.* **2011**, *33*, 1101−1105.
(66) Hoesli, C. A.; Raghuram, K.; Kiang, R. L. J.; Mocinecová, D.; Hu, X.; Johnson, J. D.; Lacík, I.; Kieffer, T. J.; Piret, J. M. *Biotechnol. Bioeng.* **2011**, *108*, 424−434.
(67) Moebus, K.; Siepmann, J.; Bodmeier, R. *Eur. J. Pharm. Biopharm.* **2009**, *72*, 42−53.
(68) Sun, X.; Shi, J.; Zhang, Z.; Cao, S. *J. Appl. Polym. Sci.* **2011**, *122*, 729−737.
(69) Işıklan, N.; İnal, M.; Kurşun, F.; Ercan, G. *Carbohydr. Polym.* **2011**, *84*, 933−943.
(70) Xing, J.; Deng, L.; Dong, A. *J. Appl. Polym. Sci.* **2010**, *117*, 2354−2359.
(71) Castro, G. R.; Kamdar, R. R.; Panilaitis, B.; Kaplan, D. L. *J. Contr. Release* **2005**, *109*, 149−157.
(72) Pearson, R. G. *J. Am. Chem. Soc.* **1963**, *85*, 3533−3539.
(73) Furia, T. E. *CRC Handbook of Food Additives*, 2nd ed.; CRC Press: Boca Raton, FL, 1972; Vol. *2*.
(74) Li, L.; Zhao, X.; Yang, C.; Hu, H.; Qiao, M.; Chen, D. *Drug Dev. Ind. Pharm.* **2011**, *37*, 1170−1180.
(75) Emami, J.; Hamishehkar, H.; Najafabadi, A. R.; Gilani, K.; Minaiyan, M.; Mahdavi, H.; Mirzadeh, H.; Fakhari, A.; Nokhodchi, A. *J. Microencapsul.* **2009**, *26*, 1−8.
(76) Kaminari, N. M. S.; Ponte, M. J. J. S.; Ponte, H. A.; Neto, A. C. *Chem. Eng. J.* **2005**, *105*, 111−115.
(77) Orhan, G.; Gezgin, G. G. *Metall. Mater. Trans., B* **2011**, *42*, 771−782.
(78) Ferreira, F. B. A.; Silva, F. L. G.; Luna, A. S.; Lago, D. C. B.; Senna, L. F. *J. Appl. Electrochem.* **2007**, *37*, 473−481.
(79) Harris, D. C. *Quantitative Chemical Analysis*, 6th ed.; W.H. Freeman: New York, 2002.
(80) Noble, J. E.; Bailey, M. J. A. *Methods Enzymol.* **2009**, *463*, 73−95.
(81) Stat-Ease, Inc. *Design-Expert User's Guide*; The Stat-Ease Inc.: Minneapolis, MN, 2001.
(82) Leardi, R. *J. Chemom.* **2003**, *17*, 569−570.
(83) Laviron, E. *J. Electroanal. Chem.* **1979**, *101*, 19−28.
(84) Laviron, E.; Roullier, L. *J. Electroanal. Chem.* **1980**, *115*, 65−74.
(85) Bard, A. J.; Faulkner, L. R. *Electrochemical Methods: Fundamentals and Applications*; Wiley: New York, 1980.
(86) *Scanning Electrochemical Microscopy*; Bard, A. J., Mirkin, M. V., Eds.; Marcel Dekker: New York, 2001.
(87) Stoica, L.; Neugebauer, S.; Schuhmann, W. In *Biosensing for the 21st Century*; Advances in Biochemical Engineering-Biotechnology; Springer: New York, 2008; Vol. *109*, pp 455−492.
(88) Sugimura, H.; Uchida, T.; Shimo, N.; Kitamura, N.; Shimo, N.; Masuhara, H. *J. Electroanal. Chem.* **1993**, *361*, 57−63.
(89) Wittstock, G.; Hesse, R.; Schuhmann, W. *Electroanalysis* **1997**, *9*, 746−750.
(90) Hess, C.; Borgwarth, K.; Ricken, C.; Ebling, D. G.; Heinze, J. *Electrochim. Acta* **1997**, *42*, 3065−3073.
(91) Grisotto, F.; Ghorbal, A.; Goyer, C.; Charlier, J.; Palacin, S. *Chem. Mater.* **2011**, *23*, 1396−1405.
(92) Actis, P.; Manesse, M.; Nunes-Kirchner, C.; Wittstock, G.; Coffinier, Y.; Boukherroubde, R.; Szunerits, S. *Phys. Chem. Chem. Phys.* **2006**, *8*, 4924−4931.
(93) Myers, R. H.; Montgomery, C. M. *Response Surface Methodology: Process and Product Optimization Using Designed Experiments*; Wiley: New York,1995.
(94) Myers, R. H.; Carter, W. H. Jr. *Technometrics* **1973**, *15*, 301−317.
(95) Box, G. E. P.; Wilson, K. B. *J. R. Statist. Soc., B* **1951**, *13*, 1−45.
(96) El Gamal, S. S.; Naggar, V. F.; Allam, A. N. *Drug Dev. Ind. Pharm.* **2011**, *37*, 855−867.
(97) Idris, A.; Suzana, W. *Process Biochem.* **2006**, *41*, 1117−1123.
(98) Brewer, G. J. *Chem. Res. Toxicol.* **2010**, *23*, 319−326.
(99) RDA - Recommended Dietary Allowance of nutritional elements: http://www.anyvitamins.com/rda.htm.
(100) Anfinsen, C. B.; Edsall, J. T.; Richards, F. M. *Advances in Protein Chemistry*; Academic Press: New York, 1985; Vol. *37*.
(101) You, J.-O.; Peng, C.-A. *J. Gene. Med.* **2005**, *7*, 398−406.
(102) Wetter, L. R.; Deutsch, H. F. *J. Biol. Chem.* **1951**, *192*, 237−242.